

## Volume 7 Paper 5

---

# The Use of SVET for Investigating Changes in the Corrosion Mechanism Induced by Forming Galvanised Steel Samples

B.P. Wilson <sup>1</sup>, D.A. Worsley <sup>2</sup>, H.N. McMurray <sup>2</sup> and J.R. Searle <sup>3</sup>

<sup>1</sup> *Max-Planck-Institut für Eisenforschung, Max-Planck-Str. 1, 40237 Düsseldorf, Germany, [wilson@mpie.de](mailto:wilson@mpie.de)*

<sup>2</sup> *Department of Materials Engineering, University of Wales, Swansea, Singleton Park Swansea, SA2 8PP, UK, [H.N.McMurray@swan.ac.uk](mailto:H.N.McMurray@swan.ac.uk)*

<sup>3</sup> *Corus Colors, Shotton Works, Deeside, Flintshire, CH5 2NH, [Justin.Searle@corusgroup.com](mailto:Justin.Searle@corusgroup.com)*

## Abstract

A novel three dimensional scanning reference electrode technique [1] (3-D SVET) apparatus is described, which uses a bi-functional probe to record topographical and current density data. This apparatus is used to investigate the effects of forming on localised current distributions as they occur at the surface of galvanealed (Zn-Fe alloy coated) sheet steel freely corroding in near neutral, aerated, aqueous chloride electrolyte. On flat samples areas anodic and cathodic currents are localised but anodic and cathodic sites occur at random over the exposed sample surface during a 24-hour immersion period. In formed samples cathodic activity remains strongly focussed on the convex portions of the exposed sample surface and anodic activity remains focused on concave portions of the exposed sample surface.

---

This is a preprint of a paper that has been submitted for publication in the Journal of Corrosion Science and Engineering. It will be reviewed and, subject to the reviewers' comments, be published online at <http://www.umist.ac.uk/corrosion/jcse> in due course. Until such time as it has been fully published it should not normally be referenced in published work. © UMIST 2004.

This effect is ascribed to iron exposure occurring through cracks in the Zn-Fe coating layer on the convex portion of the sample surface and to geometrically facilitated O<sub>2</sub> mass transport in convex regions combining to promote cathodic O<sub>2</sub> reduction.

**Keywords:** 3-D SVET, forming, galvanneal

## **Introduction**

The automotive industry uses approximately 35 million tons of steel every year. The majority of which is galvanised then formed into intricate shapes and joined in a number of ways including adhesives [2], laser [3] and resistance spot welding [4]. With increasing demands for corrosion resistance in automotive steels it is desirable to determine the effect of forming and joining on subsequent localised corrosion behaviour. The scanning vibrating electrode technique (SVET) is a well-established electrochemical technique that allows the spatial distribution of the often highly localised electrochemical reactions of corrosion to be investigated. [5] The SVET utilises a movable microtip electrode to detect the potential gradients produced by localised ionic current fluxes within the solution above a corroding surface. SVET has been used to investigate a variety of substrates including organically coated architectural steels [6] and corrosion pathways including galvanic [7] [8] [9] [10] [11] [12] and pitting corrosion [13] [14]. However, to date, the use SVET has been largely restricted to planar samples, which obviously limits its usefulness in the context of formed and joined materials. The failure of SRET in non-planar applications arises from the difficulties associated with obtaining a topographical profile of the sample, which can be subsequently utilised to accurately manoeuvre the microelectrode probe at a fixed distance above the corroding surface. Here we describe the development and use of a non-planar, three-dimensional SVET apparatus, which is simple to use and which can provide additional insight into corrosion processes occurring on formed samples of zinc coated steel for automotive use

The material we have aimed to investigate consists of a sheet steel substrate with galvanneal zinc-alloy coating. The galvanneal coating is

produced by first passing the steel sheet through a molten zinc bath containing ~0.15% aluminium by weight to produce a hot-dipped zinc coating of controlled thickness. The coated sheet is then annealed at temperatures sufficient to break down the thin aluminium-rich intermetallic layer formed during hot dipping and produce a coating consisting entirely of iron-zinc intermetallics. [15] Galvanneal is primarily used for automotive applications in both internal and external body panels. The galvanneal coating have improved spot weldability and paintability [16] [17] due to the presence of iron in the coating surface. The major drawback of galvanneal is the brittle nature of the alloy coating, which can lead to cracking, “dusting” and delamination of the coating during forming processes. [18] [19]

## **Experimental Section**

### **Materials**

Galvannealed steel of automotive grade was obtained from Corus Strip Steel Products. The 0.8mm gauge mild steel strip substrate had been coated on both sides and annealed to produce a ~10 $\mu$ m thick iron-zinc alloy layer. All chemicals were obtained in analytical grade purity from the Aldrich chemical company Ltd.

Flat 50mm x 50mm square coupons were cut from a galvannealed panel, degreased with acetone, and polished with an aqueous slurry of 0.9 $\mu$ m aluminium powder to remove any surface oxide layer. Coupons were finally rinsed with distilled water, then acetone, and allowed to dry in air. A 10mm x 10mm square area for SVET investigation was isolated in the centre of the sample surface using insulating lacquer (Lacomit) followed by PVC insulating tape, i.e. the only part of the coupon left uncoated was the area to be scanned. Domed samples were prepared by an impact former from flat coupons using a 2.5cm diameter bull nosed die with stored impact energy of 18J. After forming, a 20mm x 10mm rectangle was isolated on the dome contour and the remainder of the sample was again insulated using both Lacomit and insulating tape.

### Three Dimensional SVET

The custom built 3D-SVET apparatus is shown schematically in figure 1. The position of the SVET probe is controlled using stepper motors driving an orthogonal arrangement of linear bearings (Time and Precision Ltd.) The SVET signal was detected and digitised using an EG&G Model 5120 lock-in amplifier. Probe movement and data logging are carried out under microcomputer control. The SVET probe assembly is shown schematically in figure 2. The probe itself consists of a 125  $\mu\text{m}$  diameter platinum wire sealed in a glass tube of 250  $\mu\text{m}$  external diameter, with the end polished flat to expose a 125  $\mu\text{m}$  diameter platinum microdisc. The probe is mounted on a moving coil electromagnetic driver (vibrator) incorporating a re-entrant magnetic core. The electromagnetic driver is housed in a mu-metal enclosure to prevent magnetic flux leakage. The probe assembly was used in two modes: firstly as a contact detector (displacement mode) and secondly as an SVET electrode (SVET mode).

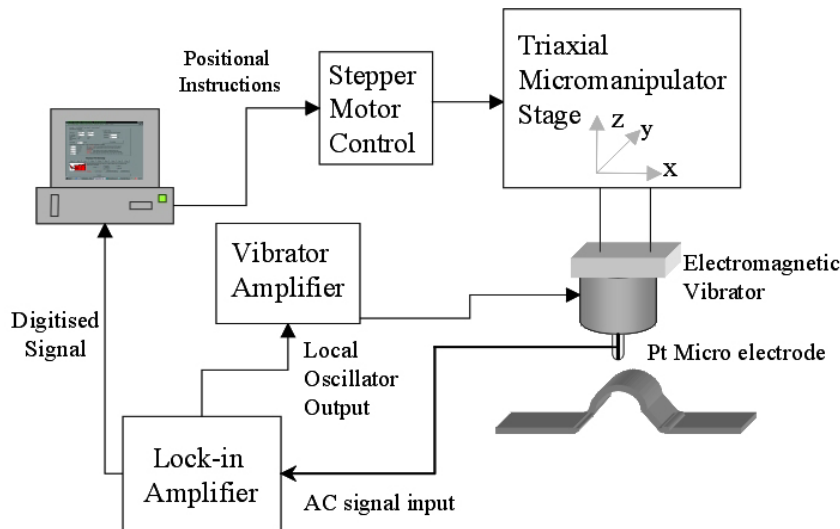


Figure 1. Schematic representation of the three dimensional SVET apparatus

#### Displacement mode

Vertical displacement of the probe electrode, as shown in figure 2B, forces the moving coil further into the re-entrant magnetic core, which has the effect of increasing coil inductance. By making the drive coil part of an inductance bridge circuit interrogated at 900Hz it is

possible to reliably detect vertical probe displacements of 2  $\mu\text{m}$ . The amplitude of the 900Hz interrogation signal is such that the amplitude of probe vibration in displacement mode is  $<1 \mu\text{m}$ . Thus, acquisition of topographical data is carried out by probe contact with the sample surface in air, i.e. before introduction of the immersion electrolyte.

Sample height at a given set of X and Y co-ordinates is measured by lowering the probe in 2 $\mu\text{m}$  increments from a known (reference) Z co-ordinate until contact is detected. On contact, the X, Y and Z co-ordinates of the probe are stored in a surface array and the process repeated for the next set of X and Y co-ordinates. It is this surface array that is used to control the position of the probe during the course of subsequent SVET scans i.e. topographical data is acquired once, in air, and used repeatedly to control SVET scans in the presence of electrolyte. This means that the time consuming process of surface profiling is carried out before the corrosion experiment commences and no time penalty is incurred during SVET scans. Furthermore, the restoring force associated with probe displacement is minimal, which ensures that profiling does not damage the sample surface.

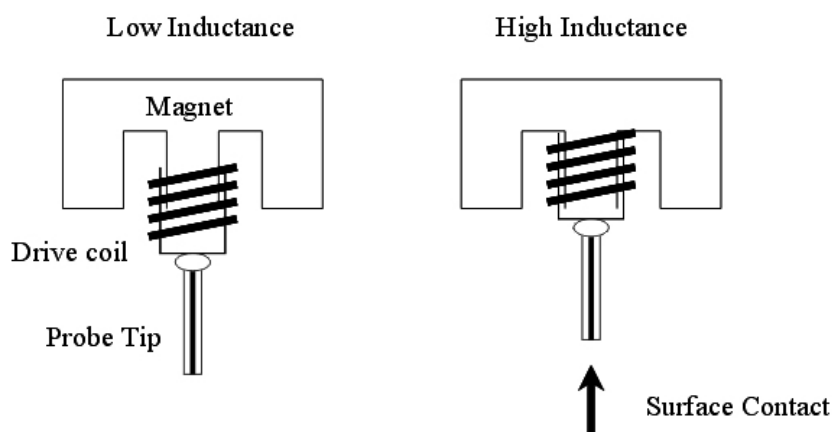


Figure 2. Schematic representation of bi-functional probe showing inductance change on vertical displacement

#### SVET Mode

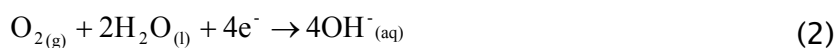
Samples were immersed in near neutral (pH6.5) 0.86 mol dm<sup>-3</sup> aerated, unstirred, aqueous NaCl at 25°C. The concentration of dissolved oxygen in the bulk solution was assumed to be constant at 2 x 10<sup>-5</sup> mol dm<sup>-3</sup>, the same as for air saturated water at this

temperature. [20] The SVET probe vibration frequency was 140Hz and the vibrational amplitude was  $\sim 40\mu\text{m}$ . All scans were conducted with the probe maintained at a constant  $100\mu\text{m}$  above the corroding surface. For the formed samples the height values were adjusted using the active Z component of the triaxial micromanipulator, which was controlled using the previously stored surface array data.

For flat samples, an array of  $40 \times 40$  SVET measurements were taken per scan to produce a mesh of 1600 data points across the  $10\text{mm} \times 10\text{mm}$  exposed sample surface. For the formed an array of  $80 \times 40$  SVET measurements were taken per scan to produce a mesh of 3200 data points across the  $20\text{mm} \times 10\text{mm}$  exposed sample surface. For both flat and formed samples the experimental period lasted for 24 hours in which the SVET apparatus performed a scan every hour.

## Results and Discussion

The most probable electrochemical processes associated with corrosion of the galvanized surface in near neutral, aerated, aqueous chloride electrolyte are anodic zinc dissolution (1) and cathodic oxygen reduction (2).



### Flat samples

Figure 3 shows a series of iso-current contour plots of the normal component of current density in the plane of scan derived from SVET scans above freely corroding flat galvanized samples. The lighter areas in these plots denote regions of net anodic activity and darker areas denote regions of net cathodic activity. It may be seen from figure 3 that anodic current distributions are highly localised, with one or more centres of anodic activity evident in every scan. Conversely, cathodic current remains more generalised throughout the course of the experiment. Localised corrosion activity of this sort is typical of galvanised steel surfaces exposed to aerated aqueous chloride electrolytes.

It is also evident from figure 3 that the location of anodic activity changes over time. This behaviour is consistent with the hypothesis that progressive dezincification of the zinc-iron alloy coating at anodic sites will lead to their eventual passivation. Anodic activity would then resume in a fresh (un-dezincified) area of the coating. Cross sections through the unformed galvaneal coating layer before and after corrosion driven de-zincification are shown in figures 4a and 4b respectively. Nevertheless, no particular pattern was observed in the evolution of anodic activity on the flat galvaneal surfaces. That is to say, anodic sites appeared to appear and disappear at random over the exposed surface and not to become concentrated in any one part of that surface.

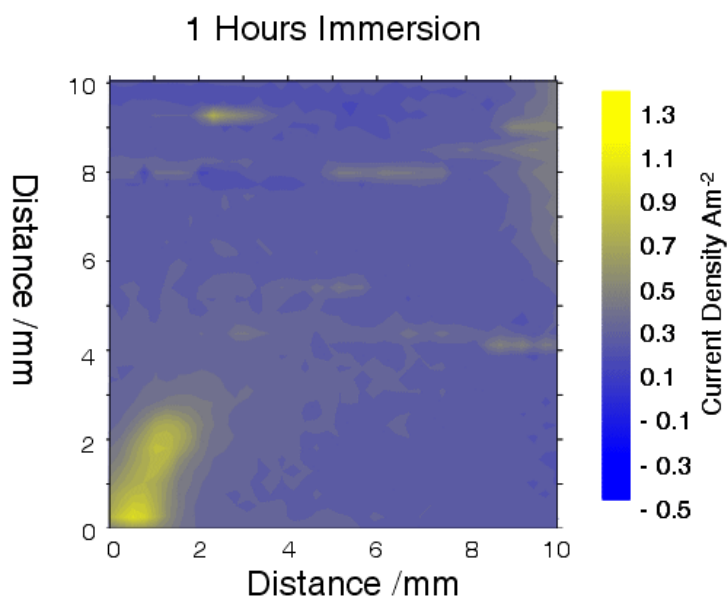
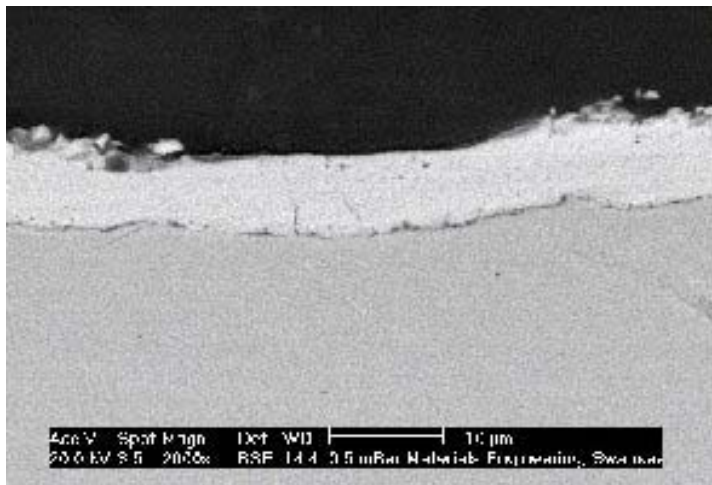
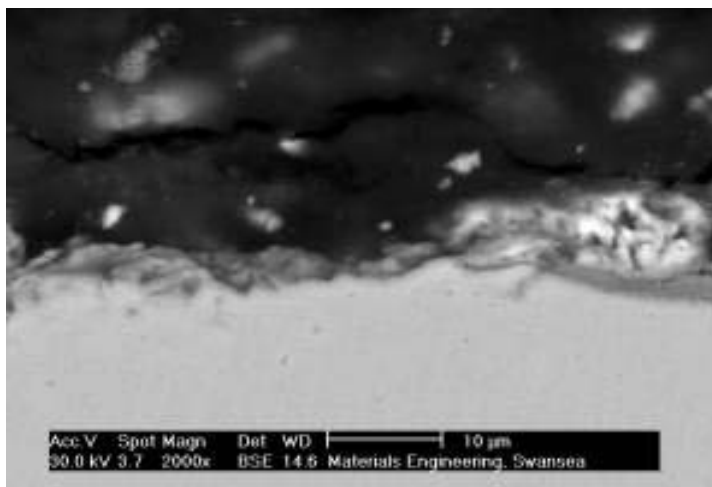


Figure 3. Iso-current contour plots of the normal component of current density derived from SVET scans above flat galvaneal samples freely corroding in  $0.86 \text{ mol dm}^{-3}$  aerated aqueous NaCl at  $20^\circ\text{C}$ .

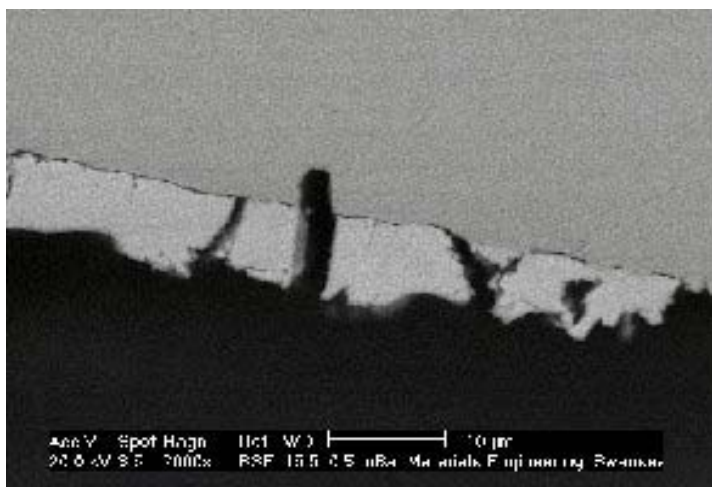
[Note that the animated GIF provided for this image does not display correctly in a PDF file. Select this [link](#) to view the animated image in your Web browser.]



a) Flat sample – before corrosion



b) Flat sample – after corrosion



c) Domed sample – before corrosion





It can be seen from figure 5 that, as in the case of the flat galvanneal sample, anodic and cathodic current distributions remain localised throughout the 24 hour experimental period. Furthermore current density values observed for the formed sample are similar to those observed in the case of the flat sample. However, in contradistinction to the flat case, the domed galvanneal sample exhibits a definite pattern in the evolution of anodic and cathodic current distributions. Figure 5 shows that the convex crown of the dome remains strongly cathodic throughout and anodic activity is concentrated on the concave dome sides. Thus it would appear that forming has significantly influenced the distribution of electrochemical activity on the sample surface.

The results shown here are of a preliminary nature and their explanation is necessarily speculative. Nevertheless, two phenomena suggest themselves as likely contributors to the observed effects. The first of these derives from the nature of the galvanneal coating itself and changes induced in its structure by the forming process. Figures 4c and 4d show cross sections through the convex portion of the domed galvanneal sample before and after corrosion respectively.

It may be seen from figure 4c that cracks have become initiated in the coating, normal to the sample surface, and that these cracks have propagated to the coating-substrate interface and in some cases into the substrate itself. This type of cracking was mainly observed on the convex portion of the formed surface. Iron is well known to exhibit a lower cathodic overpotential for reaction 2 than does zinc. Thus, increased iron exposure in convex portions of the formed sample surface may result in enhanced cathodic oxygen reduction in these regions, as shown schematically in figure 6A.

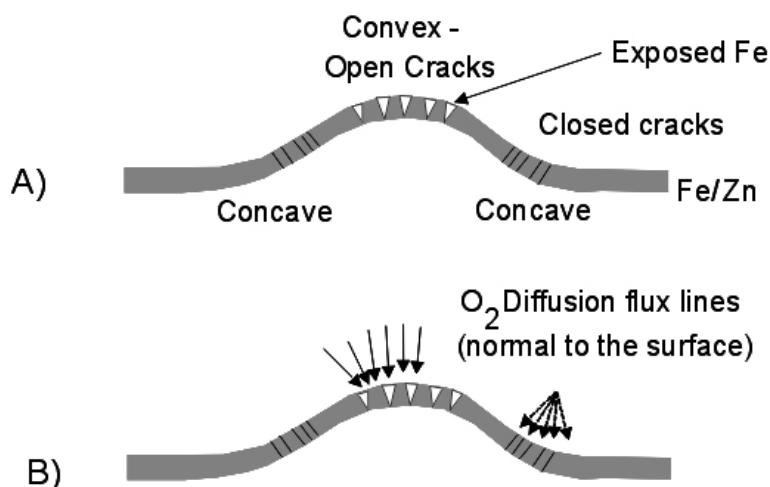


Figure 6. A) Schematic illustration of the types of cracking induced in the galvanneal coating by the forming process B) illustration of the geometry of oxygen diffusion at convex and concave portion of the sample surface.

However, for purely geometric reasons, mass transport of dissolved  $O_2$  is also likely to be more rapid to convex portions of the formed surface than to concave portions. This effect is illustrated in figure 6B, which shows lines of oxygen diffusion flux normal to the sample surface. It may be seen from figure 6B that lines of flux converge onto the convex surface but diverge onto the concave surface. Thus, it is also possible that differential aeration may contribute to the characteristic patterns of electrochemical activity seen in figure 5.

## Conclusions

We have shown that the determination of current density distributions immediately proximal to the surface of non-planar corroding samples is possible using 3-D SVET apparatus. 3-D scanning may be facilitated by using an electromagnetically driven probe, which may be used both as a displacement (contact) detector and SVET electrode. Thus, topographical data obtained in air may be used to scan the SVET probe accurately at a fixed height above the sample when immersed in electrolyte solution, without the need for probe re-alignment.

Using this apparatus we have shown that forming may significantly affect the distribution of localised anodic and cathodic electrochemical

activity occurring on Zn–Fe alloy coated sheet steel freely corroding in near neutral, aerated aqueous chloride electrolytes. Anodic activity tends to become focused on concave portions of the formed surface and cathodic activity tends to become focused on convex portions of the formed surface.

This effect is consistent with the promotion of cathodic oxygen reduction on convex portions of the exposed sample surface as a consequence of increased iron exposure at open cracks in the coating layer. However, increased rates of oxygen diffusion to the convex surface, occurring simply as a result of the geometry of the diffusion problem, may also contribute to the effect

## References

---

- 1 H.N. McMurray, J.R. Searle, B.P. Wilson, D.A. Worsley, *British Corrosion Journal*, **2002**, Vol.37 (No.3), pp225–230
- 2 The Book of Steel, Eds G. Béranger, G. Henry, G. Sanz, Lavoiser Pub., Paris 1996 Chapter 39, pp844–859
- 3 W.Waddell, G.M. Davies, *Welding & Metal Fabrication*, March 1995
- 4 The Book of Steel, Eds G. Béranger, G. Henry, G. Sanz, Lavoiser Pub., Paris 1996 Chapter 38, pp806–843
- 5 H.N. McMurray and D. A Worsley, in *Research in Chemical Kinetics*, Vol. 4, R. G. Compton and G. Hancock eds., Blackwell Science, Oxford 1997, p149
- 6 D. A. Worsley, H. N. McMurray, A. Belghazi, *Chem. Comm.*, **1997**, (024), pp2369–2370
- 7 H. S. Issacs, *J. Electrochem. Soc.*, 1991, 138, pp723
- 8 H. S. Issacs, *Advances in localised corrosion*, eds. H. Isaacs, U. Bertocci, J. Kruger and S. Smialouzka, NACE, 1988, pp221

- 
- 9 K. Komai, K. Minoshima and G. Kim, JSME Int J. Ser. I, 1989, 32, pp282
- 10 J. Hawkins, G. E. Thompson, G. C. Wood and H. S. Issacs, Abstracts of the American Chemical Society, Washington DC, 1989, pp 65
- 11 G. Pallos and G. Wallwork, Corrosion, 1982, 38, pp305
- 12 M. J. Franklin, D. C. White and H. S. Issacs, Corrosion Sci., 1992, 33, pp251
- 13 H. S. Isaacs, Corrosion Sci., 1989, 28, pp547
- 14 T. Shibata, T. Haruna and S. Fujimoto, Corrosion Eng., 1990, 39, pp331
- 15 The Book of Steel, Eds G. Béranger, G. Henry, G. Sanz, Lavoiser Pub., Paris 1996 Chapter 39, pp1281–1288
- 16 A.M. Karlson Jr, “Coated Steel Sheets in North America – An Automotive Perspective” Proceedings of the International Conference on Zinc and Zinc–Alloy Coated Steel Sheet (Galvatech), pp271–277, The Iron and Steel Institute of Japan, Tokyo, Japan 1989
- 17 B.M. Gray, C. Belleau, M.A.D. D’Amico, R.L. Pyle, J.F. Butler, “Development of Hot–Dip Zn–Fe Alloy Coated Steel for Automotive Applications”, 1989 Mechanical Working and Steel Processing Proceedings, pp3–15, ISS Warrendale, PA 1989.
- 18 The Book of Steel, Eds G. Béranger, G. Henry, G. Sanz, Lavoiser Pub., Paris 1996 Chapter 49, pp1007–1008
- 19 V. Rangarajan, Steel in Automotive Applications (SP–1259), SAE International Publications, Warrendale, PA, USA, Feb 1997, pp1–11
- 20 A. Bonnel, F. Dabosi, C. Delouis, M. Dupart, M. Kedam and B. Tribonet, J. Electrochem. Soc., 130 (1983), pp753